Est. 1984

ORIENTAL JOURNAL OF CHEMISTRY
An International Open Free Access, Peer Reviewed Research Journal

www.orientjchem.org

ISSN: 0970-020 X
CODEN: OJCHEG
2018, Vol. 34, No.(1):
Pg. 444-449

Hydration of Strontium-doped Monocalcium Aluminate

ANTI KOLONIAL PRODJOSANTOSO*, SEPTIANI, MAXIMUS PRANJOTO UTOMO, and KUN SRI BUDIASIH

Department of Chemistry, Yogyakarta State University, Yogyakarta, DIY 55281 Indonesia.
*Corresponding author E-mail: prodjosantoso@uny.ac.id

http://dx.doi.org/10.13005/ojc/340148

(Received: September 30, 2017; Accepted: November 04, 2017)

ABSTRACT

Monocalcium aluminate (CA) is the major hydraulic phase in the calcium aluminate cements (CAC). Solid solution of $Ca_{1-x}Sr_xAl_2O_4$ may be formed if the cement raw materials are impure with Sr mineral. This study aims to understand the hydration of $Ca_{1-x}Sr_xAl_2O_4$. The nature, crystallinity and microstructure of hydrated phases were identified using scanning electron microscopy (SEM-EDX), thermal gravimetric analysis (TGA), differential scanning calorimetry (DSC), X-ray diffraction (XRD) and infrared spectroscopy (IR Spectroscopy). There is a strong indication that the hydration produces a mixture of $Ca_{1-x}Sr_xAl_2(OH)_{12}$ and AH_3.

Keywords: Monocalcium aluminate, Hydration, $Ca_{1-x}Sr_xAl_2(OH)_{12}$, AH_3.

INTRODUCTION

Calcium aluminate cements (CAC) have alumina contents varying from about 38% to 90% $^w/_w$, in the form of monocalcium aluminate ($CaAl_2O_4$ or CA). Second phases include belite, corundum, dodecacalcium hepta-aluminate, ferrite pleocroite, gehlenite, monocalcium dialuminate, and wüstite. The CA is the major hydraulic reacting with water to form a series of calcium aluminate hydrates, which vary with temperature and time.[1–4]

At low temperatures (<20 °C), the main crystalline hydrate formed is CAH_{10}, and an amorphous phase is formed in considerable amounts.[5–7] This amorphous phase is usually taken to be alumina gel, but Payne & Sharp have argued that it must be one containing a calcium aluminate hydrate of unknown composition since no CH [$Ca(OH)_2$] or calcium rich aluminate hydrates are simultaneously formed to maintain a chemical balance.[8] At higher temperatures, C_2AH_8 is formed

as well as or instead of CAH_{10}. Both of these hydrates are hexagonal in morphology and thermodynamically metastable. Above 28 °C, they convert rapidly into C_3AH_6 which has a cubic structure, and gibbsite [$Al(OH)_3$ or AH_3].[7] The reactions are schematically summarized below.

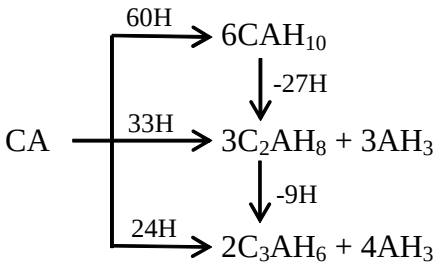

Although the presence of major hydrates, CAH_{10} [$CaAl_2(OH)_8(H_2O)_6$], C_3AH_6 [$Ca_3Al_2(OH)_{12}$] and AH_3 [$Al(OH)_3$], can be detected by X-ray diffraction (XRD), the peaks are not readily suitable for quantitative analysis. Preferred orientation can occur with hexagonal phases such as CAH_{10}, and also the hydrates may not be entirely crystalline, especially at the early stages of hydration. Also there are phases, which are amorphous by nature, e.g. the gel phases, and the presence of these will not be detected by XRD.[6,7] Therefore, the use of thermal analysis techniques is very important in the study of CA as it gives information as to the hydrate phases present in the early stages of hydration, when this may not be possible from XRD.[9]

The morphology and mechanism of crystallization of the gel phase has previously been studied by TEM.[10] Although there have been some reports about conversion reactions products in high alumina and calcium aluminate cements, but there is lack of information about the exact microstructure and growth of these phases.[11]

Solid solution of $Ca_{1-x}Sr_xAl_2O_4$ formed if the cement raw materials are impure with Sr mineral is recently investigated. Attempts have been taken to give a clear understanding of $Ca_{1-x}Sr_xAl_2O_4$ hydration, by applying different methods, such as SEM/EDX, TGA, DSC, XRD, and IR spectrometry.

EXPERIMENTAL

Polycrystalline samples of $Ca_{1-x}Sr_xAl_2O_4$ were prepared from mixtures of analytical grade $CaCO_3$ (Univar 99%), $SrCO_3$ (Merck pa.), and $Al(NO_3)_3.9H_2O$ (Aldrich 98%). For each composition the appropriate stoichiometric mixture was very thoroughly ground in an agate mortar and pestle for several minutes. The mixtures were then treated using method described by Prodjosantoso.[12,13]

Hydrated samples were prepared by adding H_2O to the finely powdered oxides in the mole ratio of 100:1.[14] The mixtures were stirred for 2 weeks under a nitrogen atmosphere at ambient temperature. The reactions were terminated by addition of acetone, and the solids were collected by filtration and then dried under a stream of dry nitrogen. The resulting materials were then characterized using Scanning Electron Microscope (Hitachi SU 3500), Thermogravimetry Analyzer (Mettler Toledo TGA-DSC 1), Powder X-Ray Diffractometer (*Shimadzu XRD-6000*), and Fourier Transform Infrared Spectrophotometer (Shimadzu IR Prestige-21).

RESULTS AND DISCUSSIONS

The hydration of $Ca_{1-x}Sr_xAl_2O_4$ was undertaken at intermediate temperature ie. at between 28 to 36 °C for 14 days. The morphologies of the unhydrated and hydrated $Ca_{1-x}M_xAl_2O_4$ samples were inspected using SEM. In general, the samples consist of non-descript shaped crystals with sizes varying in the range 0.01 to 0.1 mm. A selected SEM micrograph of the samples is displayed in Figure. 1.

EDA has been used to check the atomic composition of the samples. For the seven Sr-doped samples the Sr contents derived from the EDA analysis are systematically high, however the observed Ca:Sr:Al ratios are in reasonable agreement with the expected values (Table. 1.). EDA spectra for unhydrated and hydrated $Ca_{0.5}Sr_{0.5}Al_2O_4$ are given in Fig. 2. SEM and EDA methods were succeed to qualitative and quantitative elemental analysis but were not recognized the formation of AH_3, C_2AH_8, CAH_{10} and $Ca_{1-x}Sr_xAl_2(OH)_{12}$ in the samples.

The occurrence of AH_3, C_2AH_8, CAH_{10} and $Ca_{1-x}Sr_xAl_2(OH)_{12}$ in the hydrated samples were then confirmed by TGA-DSC thermograph, however evidences indicate the formation of AH_3 and $Ca_{1-x}Sr_xAl_2(OH)_{12}$. The TGA-DSC plot of hydrated $Ca_{0.5}Sr_{0.5}Al_2O_4$ is depicted in Fig. 3. while the thermal decompositions of hydrated $Ca_{1-x}Sr_xAl_2O_4$ are listed in Table 2.

Some samples indicate stages weight loss at temperature below 80 °C indicating evaporation of acetone used to terminate dehydration processes, and trapped in the solid samples. The rest of the stages, in general, consist of a two main stage weight loss. The first one, in the range of 250"300 °C, is attributed to the decomposition of $Al(OH)_3$, which is probably in the form of gibbsite, bayerite and nordstandite. Gibbsite, bayerite and nordstandite are dehydrated at 300, 275, and 280 ^{0}C, respectively, and are decomposed to gamma-, eta-, and eta-Al_2O_3, respectively. Broad peak at about 500 to 600 ^{0}C indicates the coarse gibbsite and bayerite, which are partially decomposed first to boehmite at 210 and 225 ^{0}C, respectively, and then to gamma-Al_2O_3 at 510 ^{0}C and eta-Al_2O_3 at 505 ^{0}C.

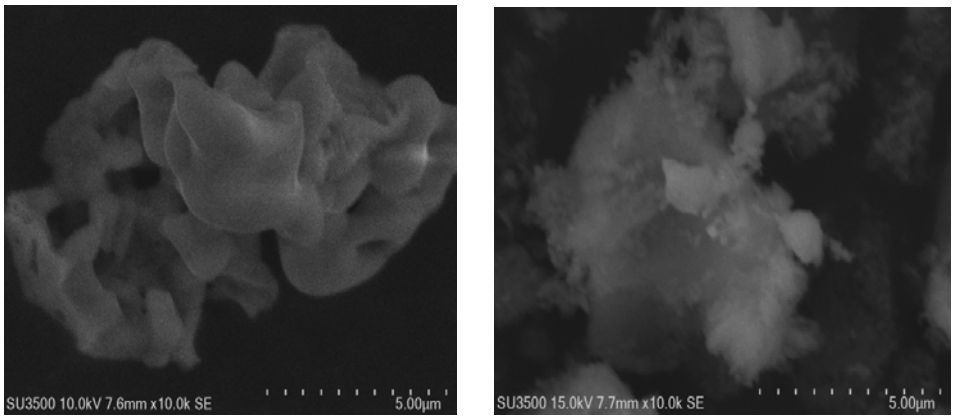

Fig. 1. SEM micrograph of unhydrated (a) and hydrated $Ca_{0.5}Sr_{0.5}Al_2O_4$(b)

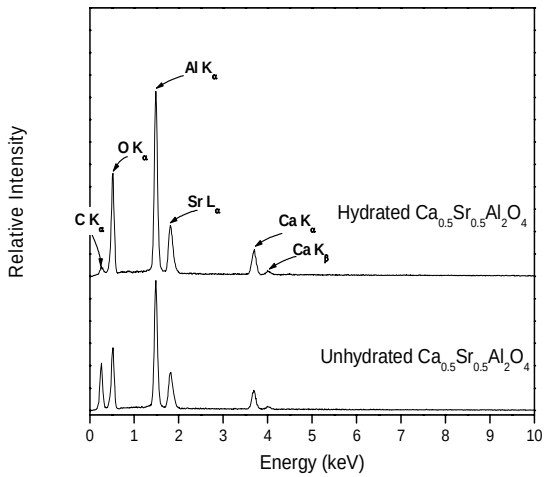

Fig. 2. EDA spectra for unhydrated and hydrated $Ca_{0.5}Sr_{0.5}Al_2O_4$

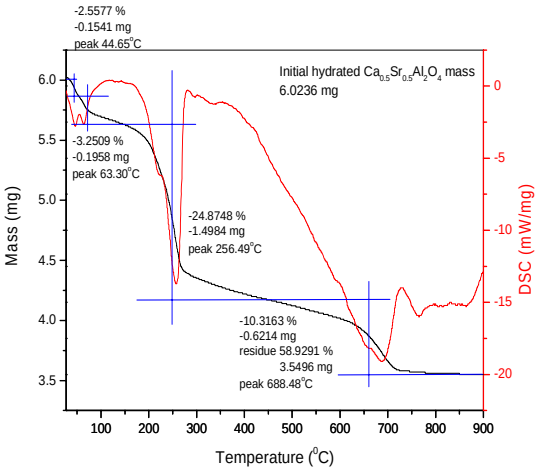

Fig. 3. The TGA-DSC plot of hydrated $Ca_{0.5}Sr_{0.5}Al_2O_4$

The characteristic feature of amorphous $Al(OH)_3$ phase such as the gradually changing and step-less weight loss curve and the broad DSC endothermic structure between 200 ^{0}C and 500 ^{0}C is confirmed. This supports the conclusion that the hydrated samples contain amorphous $Al(OH)_3$ as

major species. The weak endotherms at about 250 ^{0}C and 420 ^{0}C represent amorphous $Al(OH)_3$ to amorphous Al_2O_3 decomposition.

It is difficult to estimate the relative amounts of amorphous $Al(OH)_3$ in the sample based on the DSC endothermic peaks. When a sample is a mixture of different chemical species, and the weight change is much slower due to, for example, release of strongly adsorbed water, than the temperature ramping rate, its DSC curve does not necessarily show their endo- and exo-therms at the same temperatures and can be weakened and broadened. A DSC peak height is not often related to the amount of the weight loss. If the weight decreases linearly with increasing temperature, the DSC curve will look flat although there is a weight loss. However, the TGA data seems to suggests that $Al(OH)_3$ is a major species.

Table. 1: Atomic ratio of $Ca_{1-x}Sr_xAl_2O_4$ (e.s.d. ± 0.005).

$Ca_{1-x}Sr_xAl_2O_4$, x =	Atoms		
	Ca	Sr	Al
0	1.01	0	1.99
0.125	0.90	0.16	1.94
0.25	0.75	0.30	1.95
0.5	0.46	0.55	1.98
0.75	0.19	0.79	2.02
0.875	0.14	0.86	2.00
1	0	1.06	1.94

The main loss of water occurred at around 300 °C indicates the presence of $Ca_{1-x}Sr_xAl_2(OH)_{12}$. The water loss of up to 350 °C equals to approximately $5H_2O$. The total water loss up to 600 °C (28 wt.%) is consistent with the presence of 6 waters in $Ca_{1-x}Sr_xAl_2(OH)_{12}$, similar to C_3AH_6.[15] These crystalline powders also show sharp endothermic peaks and stepwise weight losses at 300 to 600 ^{0}C. Structural analyses suggested the following decomposition processes for $Ca_{1-x}Sr_xAl_2(OH)_{12}$ in air:

$$Ca_{1-x}Sr_xAl_2(OH)_{12} \rightarrow Ca_{1-x}Sr_xAl_2O_6.2H_2O + 4H_2O \quad (262\text{-}326\ ^\circ C)$$

$$Ca_{1-x}Sr_xAl_2O_6.2H_2O \rightarrow Ca_{1-x}Sr_xAl_2O_6.H_2O + H_2O \quad (400\ ^\circ C)$$

$$Ca_{1-x}Sr_xAl_2O_6.H_2O \rightarrow Ca_{1-x}Sr_xAl_2O_6 + H_2O \quad (>600\ ^\circ C)$$

There is no evidence of mass loses between 350°C to 550 °C indicating the absence of the $Ca(OH)_2$ and or $Sr(OH)_2$ decompositions.[1617]

The crystalline phases present in the unhydrated and hydrated $Ca_{1-x}M_xAl_2O_4$ samples

Table. 2: Thermal decomposition of hydrated $Ca_{1-x}Sr_xAl_2O_4$

Compounds	Thermal decomposition			Residue
	(%)	(mg)	(°C)	
Hydrated $CaAl_2O_4$	-3.3750	-0.1916	60.76	60.4499 %
(5.6762 mg)	-22.0846	-1.2536	250.95	3.4313 mg
	-14.1532	-0.8034	702.02	
Hydrated $Ca_{0.75}Sr_{0.25}Al_2O_4$	-20.6942	-1.2414	281.10	61.6984 %
(5.9988 mg)	-17.6154	-1.0567	709.86	3.7012 mg
Hydrated $Ca_{0.5}Sr_{0.5}Al_2O_4$	-2.5577	-0.1541	44.65	58.9291 %
(6.0236 mg)	-3.2509	-0.1958	63.30	3.5496 mg
	-24.8748	-1.4984	256.49	
	-10.3163	-0.6214	688.48	
Hydrated $Ca_{0.1}Sr_{0.9}Al_2O_4$	-5.0147	-0.3007	53.00	58.4119 %
(5.9957 mg)	-3.9761	-0.2384	69.47	3.5022 mg
	-29.8422	-1.7892	253.79	
	-2.6644	-0.1597	680.43	
Hydrated $SrAl_2O_4$	-21.9251	-1.3031	281.99	68.1024 %
(5.9433 mg)	-10.0172	-0.5953	805.64	4.0475 mg

were investigated using XRD method. The X-ray diffraction pattern peak height and 2 theta position measurements of unhydrated and hydrated $Ca_{1-x}M_xAl_2O_4$ are graphically shown in Fig. 4. The different of both patterns indicates that all unhydrated samples were hydrated completely producing different phases.

Similar to C_3AH_6, the crystalline $Ca_{1-x}Sr_xAl_2(OH)_{12}$ is thermodynamically stable in the temperature range from 20 to 250 °C,[18,19] allowing this hydroxide be analyzed using XRD method. The XRD pattern of the samples prepared from $Ca_{1-x}M_xAl_2O_4$ in the present study shows the crystalline $Ca_{1-x}Sr_xAl_2(OH)_{12}$ indicated by a strong reflection at 2θ at about 17.27°. Minor peaks were observed, which could be assigned to $Al(OH)_3$ crystalline phases.

FTIR has been used to collect evidences supporting the presence of $Ca_{1-x}Sr_xAl_2(OH)_{12}$ and AH_3 in the hydrated $Ca_{1-x}Sr_xAl_2O_4$. The FTIR spectra of selected hydrated samples are depicted in Figure 6, and the IR frequencies are listed in Table. 3.

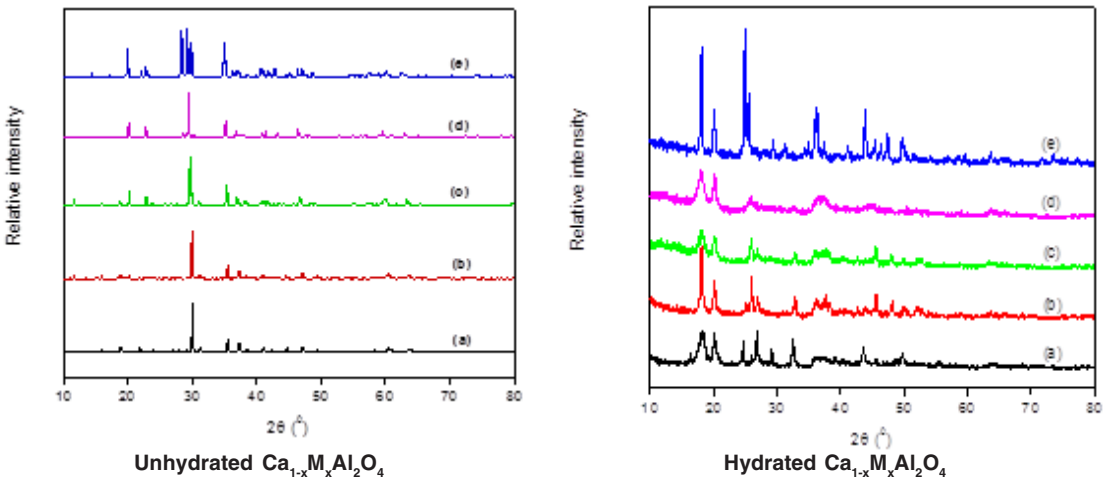

Unhydrated $Ca_{1-x}M_xAl_2O_4$ **Hydrated $Ca_{1-x}M_xAl_2O_4$**

Fig.4. Powder XRD patterns of unhydrated and hydrated of $Ca_{1-x}M_xAl_2O_4$, x = 0 (a), 0.25 (b), 0.5 (c), 0.9 (d), and 1 (e).

The formation of $Ca_{1-x}Sr_xAl_2(OH)_{12}$ could take place at the presence of a low concentration of OH^-, e.g. pH = 7-8. In basic systems, the solubility of $Al(OH)_3$ is quite large.

High solubility of the ionic species favors a large amount of hydrated ions releasing for participation in the homogeneous formation reaction; this also eliminates the chance for the occurrence of impurities. On the other hand, highly crystalline $Ca_{1-x}Sr_xAl_2(OH)_{12}$ can be formed in wider ranges of input concentrations. In the corresponding IR spectrum in Fig. 5., the absorption band at *ca.* 3600 cm^{-1} assigned to-OH stretching vibration of the lattice -OH in $Ca_{1-x}Sr_xAl_2(OH)_{12}$, and the bands at *ca.* 3450 and 1600 cm^{-1} assigned to-OH stretching and bending vibrations, respectively, in adsorbed water were also observed.[20,21]

The absorptions at about 850 cm^{-1} and 913 cm^{-1} are the characteristic absorption of the Al-O stretching bond.[22] The absorption at 1030 cm^{-1} is assigned to Al-OH bond. The weak absorption at 666 cm^{-1} is the absorption of CaO, Sr-O bonds or the combination of both of the compounds $Ca_{1-x}Sr_xAl_2(OH)_{12}$. The complete IR frequencies of hydrated $Ca_{1-x}Sr_xAl_2O_4$ is displayed in Table. 3.

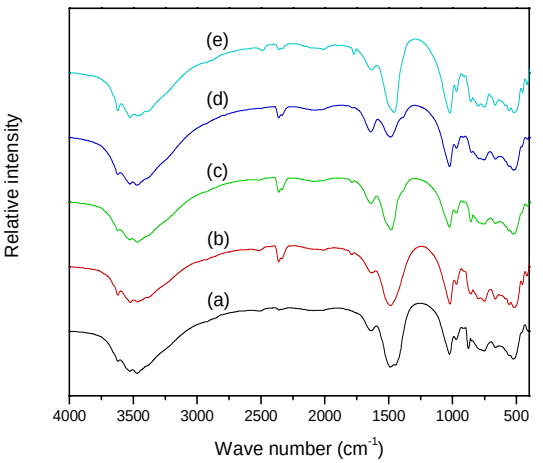

Fig. 5. The FTIR spectra of selected hydrated $Ca_{1-x}Sr_xAl_2O_4$ samples

Table. 3: The IR frequencies of hydrated $Ca_{1-x}Sr_xAl_2O_4$

Type of bond	Frequencies (cm^{-1})				
	Hydrated $CaAl_2O_4$	Hydrated $Ca_{0.75}Sr_{0.25}Al_2O_4$	Hydrated $Ca_{0.5}Sr_{0.5}Al_2O_4$	Hydrated $Ca_{0.1}Sr_{0.9}Al_2O_4$	Hydrated $SrAl_2O_4$
Al-O stretching	852.59	852.82	856.93	857.95	857.74
	913.17	913.91	915.35	913.96	913.36
Al-OH bending	1022.86	1024.20	1024.99	1020.81	1022.06
Al-OH stretching	3525.73	3526.14	3525.63	3523.33	3523.98
Ca-O, Sr-O stretching	663.38	666.07	664.80	666.31	667.74
O-H bending	1637.61	1641.65	1638.63	1632.65	1634.99
O-H stretching	3469.78	3469.13	3468.14	3465.63	3461.86

CONCLUSION

The hydration of $Ca_{1-x}Sr_xAl_2O_4$ solid solution for 14 days at ambient temperature produces a mixture of crystalline $Ca_{1-x}Sr_xAl_2(OH)_{12}$ and very poorly crystalline AH_3. Crystalline phases of $Ca(OH)_2$ and $Sr(OH)_2$ are not observed in the hydrated $Ca_{1-x}Sr_xAl_2(OH)_{12}$.

REFERENCE

1. Stinnessen, I.; Buhr, A.; Kockegey-lorenz, R.; Racher, R., *Tech. Pap.,* **2001**.
2. Scrivener, K., *Advanced Concrete Technology.,* **2003,** 1–31.
3. Scrivener, K. L.; Cabiron, J. L.; Letourneux, R., *Cem. Concr. Res.*, **1999**, *29***,** 1215–1223. DOI: 10.1016/S0008-8846(99)00103-9.
4. Pollmann, H.; Kaden, R., *Fentiman CH, Mangabhai RJ Scrivener KL.,* **2014***,* 18–21.
5. Antonoviè, V.; Keriene, J.; Boris, R.; Aleknevièius, M., *Procedia Engineering.,* **201**3, *57***,** 99–106.
6. Wang, P.; Xu, L., *Procedia Eng.,* **2017,** *27***,** 253–260.
7. Klaus, S. R.; Neubauer, J.; Goetz-Neunhoeffer, F., *Cem. Concr. Res.,* **2013**, *43***,** 62–69. DOI: 10.1016/j.cemconres., **2012**. 09.005.
8. Payne, D. R.; Sharp, J. H., *The Microstructure and Chemistry of Cement and Concrete.,* **1989**.
9. Bushnell-Watson, S. M.; Sharp, J. H., *Cem. Concr. Res.,* **1990**, *20***,** 677.
10. Richardson, I. G.; Skibsted, J.; Black, L., Kirkpatrick, R. J., *Adv. Cem. Res.,* **2010**, *22***,** 233–248. DOI: 10.1680/adcr.2010.22.4.233.
11. Rashid, S.; Turrillas, X.; *Thermochim. Acta,* **1997**, *302***,** 25–34.
12. Prodjosantoso, A., Kennedy, B., *Mater. Res. Bull.,* **2003**, *38***,** 79–87. DOI: 10.1016/S0025-5408(02)01009-7.
13. Prodjosantoso, A. K.; Kennedy, B. J.; *J. Solid State Chem.,* **2002**, *168***,** 229–236. DOI: 10.1006/jssc.2002.9715.
14. Prodjosantoso, A. K.; Kennedy, B. J.; Hunter, B. A.; *Cem. Concr. Res.,* **2002**, *32***,** 647–655. DOI: 10.1016/S0008-8846(01)00737-2.
15. Dilnesa, B. Z.; Lothenbach, B.; Renaudin, G.; Wichser, A.; Kulik, D., *Cem. Concr. Res.,* **2014**. *59***,** 96–111. DOI: 10.1016/j.cemconres. 2014. 02.001 .
16. Kim, T.; Olek, J.; *Transp. Res. Rec. J. Transp. Res. Board,* **2012**, *2290***,** 10–18. DOI: 10.3141/***2290***-02.
17. Tangy, A.; Pulidindi, I. N.; Gedanken, A.; *Energy & Fuels*, **2016**, *30***,** 3151–3160. ***DOI***: 10.1021/acs.energyfuels.6b00256.
18. Ball, M. C.; *Cem. Concr. Res.,* **1976**, *6***,** 419–420.
19. Plank, J.; Zhang-Preâe, M.; Ivleva, N. P.; Niessner, R., *Constr. Build. Mater.*, **2016**, *122***,** 426–434. DOI: 10.1016/j.conbuildmat. 2016. 06.042.
20. Kolesov, B. A.; Geiger, C. A., *Am. Mineral.,* **2005**, *90***,** 1335–1341. DOI: 10.2138/***am***. 2005.1622.
21. Saikia, B. J.; Parthasarathy, G., *J. Mod. Phys.,* **2010**, *1***,** 206–210. DOI: 10.4236/ jmp.2010.14031.
22. Torréns-Martín, D.; Fernández-Carrasco, L.; Martínez-Ramírez, S., *Cem. Concr. Res.,* **2013**, *47***,** 43–50. DOI: 10.1016/j.*cemconres*. 2013.01.015.